

# DETECTION WITH RHESSI OF HIGH FREQUENCY X-RAY OSCILLATIONS IN THE TAIL OF THE 2004 HYPERFLARE FROM SGR 1806-20

ANNA L. WATTS<sup>1,2</sup> AND TOD E. STROHMAYER<sup>1,3</sup>

*Draft version May 15, 2006*

## ABSTRACT

The recent discovery of high frequency oscillations in giant flares from SGR 1806-20 and SGR 1900+14 may be the first direct detection of vibrations in a neutron star crust. If this interpretation is correct it offers a novel means of testing the neutron star equation of state, crustal breaking strain, and magnetic field configuration. Using timing data from RHESSI, we have confirmed the detection of a 92.5 Hz Quasi-Periodic Oscillation (QPO) in the tail of the SGR 1806-20 giant flare. We also find another, stronger, QPO at higher energies, at 626.5 Hz. Both QPOs are visible only at particular (but different) rotational phases, implying an association with a specific area of the neutron star surface or magnetosphere. At lower frequencies we confirm the detection of an 18 Hz QPO, at the same rotational phase as the 92.5 Hz QPO, and report the additional presence of a broad 26 Hz QPO. We are however unable to make a robust confirmation of the presence of a 30 Hz QPO, despite higher countrates. We discuss our results in the light of neutron star vibration models.

*Subject headings:* stars: magnetic fields—pulsars: individual (SGR 1806-20)—stars: neutron—stars: rotation—stars: oscillations—X-rays: stars

## 1. INTRODUCTION

The Soft Gamma Repeaters (SGRs), objects that exhibit recurrent bouts of gamma-ray flare activity, are thought to be magnetars - neutron stars with magnetic fields greater than  $10^{14}$  G (Duncan & Thompson 1992; Thompson & Duncan 1995; Woods & Thompson 2004). On rare occasions SGRs exhibit giant flares, hugely energetic events with peak fluxes in the range  $10^{44} - 10^{46}$  ergs  $s^{-1}$ . The giant flares consist of a short spectrally hard initial peak, followed by a softer decaying tail lasting a few hundred seconds. Pulsations with periods of several seconds are visible in the tail, and reveal the neutron star spin period. Their presence is thought to be due to a fireball of ejected plasma, trapped near the stellar surface by the strong magnetic field (Thompson & Duncan 1995).

Three giant flares have been detected since the advent of satellite-borne high energy detectors: in 1979, from SGR 0526-66 (Mazets et al. 1979); in 1998, from SGR 1900+14 (Hurley et al. 1999); and in 2004 from SGR 1806-20 (Terasawa et al. 2005; Palmer et al. 2005). The catastrophic magnetic instability that powers the giant flares is thought to be associated with large-scale fracturing of the neutron star crust (Flowers & Ruderman 1977; Thompson & Duncan 1995, 2001; Schwartz et al. 2005). This will almost certainly excite global seismic vibrations (Duncan 1998): terrestrial seismologists regularly observe such global modes after large earthquakes such as the 2004 Sumatra-Andaman event (Park et al. 2005).

The 2004 flare from SGR 1806-20 was the most energetic ever recorded. Analysis of data from the *Rossi X-ray Timing Explorer* (RXTE) by Israel et al. (2005)

revealed a transient 92.5 Hz Quasi-Periodic Oscillation (QPO) in the tail of the flare, associated with a particular rotational phase. The presence of 18 and 30 Hz features was also suggested, although with lower significance. Israel et al. (2005) suggested that the 30 Hz and 92.5 Hz QPOs might be toroidal shear vibrations of the crust (Schumaker & Thorne 1983; McDermott et al. 1988; Strohmayer 1991; Duncan 1998; Piro 2005). These modes are particularly promising in terms of both ease of excitation and coupling to the magnetic field to modulate the X-ray lightcurve (Blaes et al. 1989).

Motivated by this work, Strohmayer & Watts (2005) re-analysed RXTE data for the 1998 flare from SGR 1900+14. QPOs were found at 28, 54, 84 and 155 Hz, again associated with a particular rotational phase. These QPOs can plausibly be identified with a series of toroidal modes. The association with a rotational phase away from the main peak (where emission from the surface is obscured by the trapped fireball) implies that we are seeing emission from a particular area of the stellar surface or bundle of magnetic field footpoints.

The frequencies of crustal modes such as the toroidal modes depend on neutron star mass and radius, crustal rigidity, and magnetic field configuration (Duncan 1998). For this reason the high frequency QPOs offer a powerful new diagnostic of neutron star properties provided that an accurate mode identification can be made (see Strohmayer & Watts (2005) for an initial attempt to constrain SGR parameters).

In this paper we present a timing analysis of the SGR 1806-20 hyperflare using data from the *Ramaty High Energy Solar Spectroscopic Imager* (RHESSI), and discuss our results in the light of the crustal vibration model.

## 2. OBSERVATIONS AND DATA ANALYSIS

RHESSI is a solar-pointing satellite whose primary objective is the study of solar flares in the energy range 3 keV - 17 MeV (Lin et al. 2002). The detection system comprises nine cryogenically-cooled Germanium detec-

arXiv:astro-ph/0512630 v2 9 Mar 2006

<sup>1</sup> Exploration of the Universe Division., NASA/GSFC, Greenbelt, MD 20771

<sup>2</sup> Current address: Max Planck Institut für Astrophysik, Karl-Schwarzschild-Str.1, 85748 Garching, Germany; anna@mpa-garching.mpg.de

<sup>3</sup> Email: stroh@milkyway.gsfc.nasa.gov

tors, divided into front and rear segments. For solar flares all direct photons under 100 keV should be stopped in the front segments. Most direct photons above 100 keV are captured in the higher volume rear segments. Lower energy photons reach the rear detectors only indirectly, by scattering (there is a Beryllium scatterer embedded in the front segments, intended for use in polarization studies). The rear segments also capture albedo flux from the Earth.

The SGR 1806-20 hyperflare was  $\approx 5^\circ$  off-axis for RHESSI (Boggs et al. 2004). The detector saturated during the peak, but recorded the decaying tail in its entirety (Hurley et al. (2005); Figure 1). Although the flare was not directly in the RHESSI field of view, most photons in the front segments would have been direct. Given RHESSI's native time resolution of 1 binary  $\mu$ s ( $2^{-20}$ s) these events are clearly suitable for high frequency timing analysis. The rear segment flux, by contrast, comprises scattered photons from the front segments, direct photons entering through the walls of the spacecraft, and albedo flux. The latter, which could be as much as 40-50% of the direct flux in the energy range of interest (McConnell et al. 2004), has a severe impact on timing analysis. At the time of the flare RHESSI was passing the limbs of the Earth (as viewed from the SGR). Albedo flux is limb-brightened, particularly if the incoming flux is polarized (Willis et al. 2005). This means that a large fraction of the detected photons could have incurred additional delays of up to  $\approx 0.02$  s, smearing out signals above  $\approx 50$  Hz. Note that although countrates in the rear segments exceed those recorded by RXTE, countrates in the front segments are slightly lower. It should also be noted that scattering from the spacecraft walls and the Earth will cause the photon energies recorded by RHESSI, particularly in the rear segments, to deviate from the true energies of the incident photons. Quantifying this effect precisely is extremely difficult. For this reason we use broad energy bands in our analysis, and urge some care in interpreting the recorded photon energies.

We started by extracting event lists from the RHESSI data, excluding only events occurring in a 2s period  $\approx 270$ s after the peak of the flare when an attenuator is removed (the associated spike introduces spurious variability, particularly in the front segments). Timing analysis was carried out using the  $Z_n^2$  statistic (Buccheri et al. 1983; Strohmayer & Markwardt 1999). Israel et al. (2005) showed that the presence of the high frequency signals was dependent on the phase of the 7.6s rotational pulse; the signals appeared most strongly at phases away from the main peak. Similar phase-dependence was also observed in the SGR 1900+14 hyperflare (Strohmayer & Watts 2005). As such we have conducted a phase-dependent analysis.

We searched for phase-dependent QPOs by folding data of a given rotational phase from  $N_p$  pulses, generating power spectra that are averaged to a frequency resolution  $\Delta\nu$ . The distribution of noise powers is a  $\chi^2$  distribution with  $2N$  degrees of freedom, where  $N = N_p \Delta\nu P \Delta\Phi$ ,  $P$  is the rotational period and  $\Delta\Phi$  is the phase window under consideration ( $0 < \Delta\Phi \leq 1$ ). We searched over a range of  $\Delta\Phi$ ,  $N_p$ , and energy bands for any signals with significance  $> 3\sigma$ .

We started by searching for signals in the range 50-

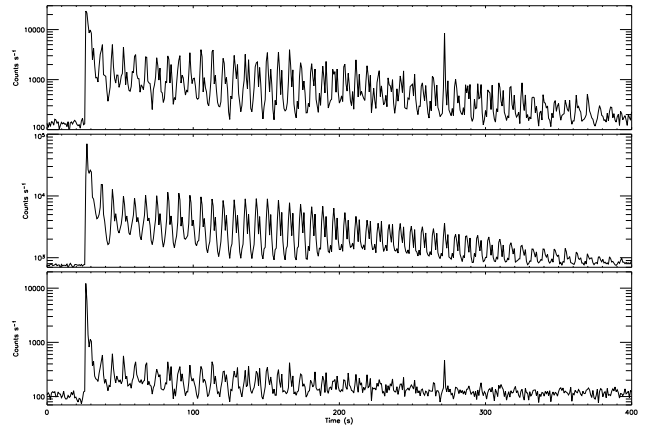


FIG. 1.— Light curves. Top: Front segments, 25-100 keV band. Center: Rear segments, 25-100 keV band. Bottom: Front segments, 100-200 keV band. The plots show the main peak and decaying tail with the 7.6s double-peaked pulse profile. The spike in the front segments at 270s is due to the removal of an attenuator. Zero time corresponds to 21:30 UTC on December 27 2004.

1000 Hz, using only data from the front segments. In this range the noise profile is Poissonian. We find only two signals that meet our search criterion.

The first, for photons with recorded energies in the range 25-100 keV, is the QPO at 92.5 Hz previously reported by Israel et al. (2005), shown in Figure 2. This signal, which we detect only at a rotational phase away from the main peak, is strongest  $\approx 150 - 260$  s after the initial flare. As noted by Israel et al. (2005), this occurs in conjunction with an increase in unpulsed emission. At  $\Delta\nu = 1$  Hz the QPO is resolved; at  $\Delta\nu = 2$  Hz it is not. We estimate the significance of the  $\Delta\nu = 2$  Hz power using a  $\chi^2$  distribution with 68 degrees of freedom, which is the distribution expected based on the number of independent frequency bins and pulses averaged. The peak at 93 Hz has a single trial probability of  $2 \times 10^{-7}$ . Applying a correction for the number of frequency bins, independent time periods, and rotational phases searched we arrive at a significance of  $\approx 1 \times 10^{-3}$ . That this is lower than the significance reported by Israel et al. (2005) is to be expected, given that the RHESSI front segment countrate is lower than that of RXTE. A search for the signal in the RHESSI rear segments indicates that the signal has indeed been smeared out due to albedo flux. Fitting the QPO with a Lorentzian profile we find a centroid frequency  $92.7 \pm 0.1$  Hz, with coherence value  $Q$  of 40. The integrated RMS fractional amplitude is  $10 \pm 0.3$  %, in good agreement with Israel et al. (2005).

The independent detection with RHESSI of the 92.5 Hz QPO is a strong confirmation of the RXTE findings. Using the significance quoted by Israel et al. (2005), we can compute the probability of getting two apparent detections at the same frequency, time and phase, due to noise alone, given the number of trials. If we do this we find that the detection of the 92.5 Hz QPO has a combined significance of  $> 6\sigma$ , an extremely robust result.

The second detection, for photons with recorded energies in the range 100-200 keV, is of a narrower QPO at 626.5 Hz (Figure 3). This signal is strongest in the period

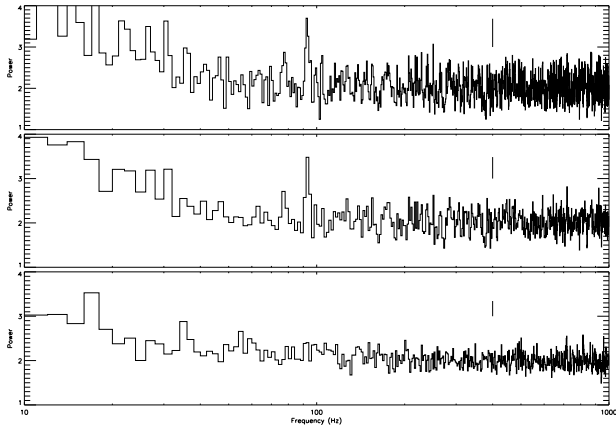


FIG. 2.— Average power spectra from 2.27 s intervals (0.3 cycles) centered on different rotational phases, computed using photons from the front segments with recorded energies in the range 25–100 keV. The upper curve was computed using 15 successive 2.27 s intervals,  $\approx 150 - 260$  s after the main flare, at a rotational phase that includes the secondary peak and part of the DC phase. The frequency resolution is 1 Hz. The middle curve shows the same spectrum with 2 Hz frequency resolution. The QPO at 92.5 Hz is clearly visible. The lower curve is for the same time period but is an average of rotational phases  $\pm 2.27$  s away from the 92.5 Hz signal phase: no QPOs are detected. Characteristic error bars are shown for each spectrum.

50–200 s after the main flare. As before, the signal is only detected at certain rotational phases; but in this case the rotational phase where the signal is strongest is centered on the leading edge of the main peak (Figure 4). We estimate the significance of the peak using a  $\chi^2$  distribution with 114 degrees of freedom, which is the distribution expected based on the number of independent frequency bins and pulses averaged. The peak at 626.5 Hz has a single trial probability of  $7.7 \times 10^{-9}$ . Applying a correction for the number of frequency bins, independent time periods, and rotational phases searched we arrive at a probability of chance occurrence of  $\approx 6.6 \times 10^{-5}$ . Fitting the QPO with a Lorentzian profile we find a centroid frequency  $626.46 \pm 0.02$  Hz, with coherence value  $Q$  of 790. The integrated RMS fractional amplitude is high, at  $20 \pm 3$  %.

Extending our search to lower frequencies, in the range 1–50 Hz, we can now use data from both the front and rear segments. In this range the noise spectrum is not Poissonian. If we focus only on the time period 200–300 s after the main flare, where Israel et al. (2005) reported possible QPOs at 18 and 30 Hz, we do not find features that meet our search criterion. Extending our search to earlier times, however, we do find evidence for low frequency features at the rotational phase where the 92.5 Hz QPO was found (Figure 5). At 1 Hz resolution we find broad features at  $\approx 18$  and 26 Hz, with a slightly weaker feature at  $\approx 30$  Hz. Assigning a significance to these putative detections requires us to fit the noise powers. We fit a constant plus power law model, excluding the candidate peaks to avoid biasing the fit. We then divide by the continuum model and multiply by 2 to obtain the normalised spectrum shown in the lower panel of Figure 5. We compute significances using a 2 Hz resolution power

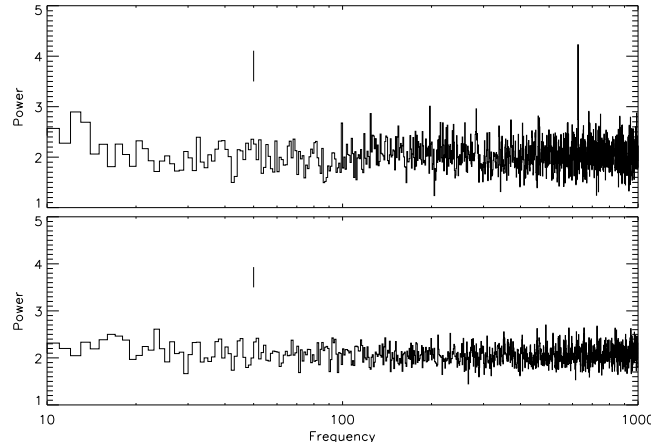


FIG. 3.— Average power spectra from 2.27 s intervals (0.3 cycles) centered on different rotational phases, computed using photons from the front segments with recorded energies in the range 100–200 keV. The upper curve was computed using 19 successive 2.27 s intervals,  $\approx 50 - 200$  s after the main flare, for a rotational phase centered on the main peak. The frequency resolution is 1 Hz, and the QPO is clearly visible at 626.5 Hz. The lower curve is for the same time period but is an average of rotational phases  $\pm 2.27$  s away from the main peak: no QPOs are detected. Characteristic error bars are shown for each spectrum.

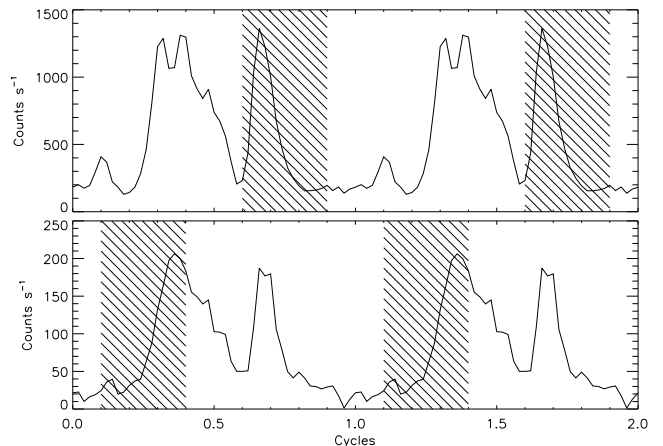


FIG. 4.— Folded pulse profiles (background subtracted), showing the rotational phase where the high frequency QPOs are detected. The top panel shows the average pulse profile for photons from the front segments, in the 25–100 keV band, for the period where the 92.5 Hz QPO is detected most strongly (2 full cycles are shown). The lower panel shows the average pulse profile for photons from the front segments, in the 100–200 keV band, for the period when the 626.5 Hz QPO is detected most strongly. The hatched regions indicate the rotational phases where the QPOs are detected.

spectrum (not shown), to take into account the breadth of the candidate QPOs. If we neglect the uncertainty associated with the normalisation, and assume that the noise is Poisson, the single trial probabilities of the powers measured at 18 Hz and 26 Hz are  $3.9 \times 10^{-8}$  and  $2.7 \times 10^{-9}$  respectively. Accounting for the number of trials, the probabilities of chance occurrence are  $8.8 \times 10^{-6}$  for the 18 Hz QPO and  $6.1 \times 10^{-7}$  for the 26 Hz QPO. The uncertainty associated with the noise model will reduce the quoted significances by some factor, but unless the

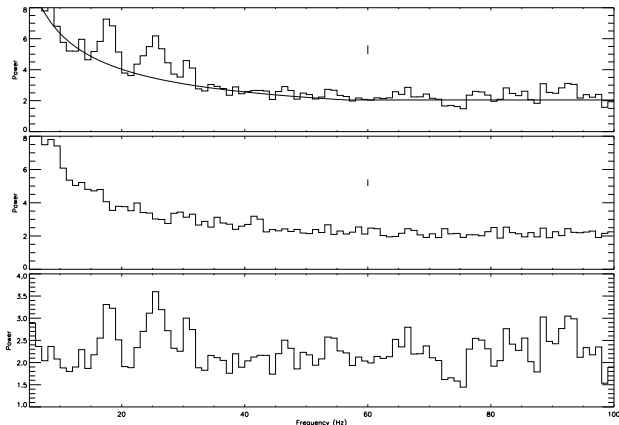


FIG. 5.— Average power spectra from 2.27 s intervals (0.3 cycles) centered on different rotational phases, computed using photons from the front and rear segments with recorded energies in the range 25–100 keV. The upper curve was computed using 22 successive 2.27 s intervals,  $\approx 60 - 230$  s after the main flare, for the rotational phase where the 92.5 Hz QPO is observed. Several possible QPOs are apparent at low frequencies, and we show the best-fit power law plus constant model of the continuum. The center curve is for the same time period, but is an average of rotational phases  $\pm 2.27$  s away from the main peak: no QPOs are detected. In the lower panel we have renormalised the power spectrum using the continuum model. Broad QPOs at 18 Hz and 26 Hz are readily apparent, as is a weaker feature at 30 Hz. Note that there is no longer a distinct QPO peak at 92.5 Hz, as there was in Figure 2, although there is a broader feature at this frequency. The fact that the peak at 92.5 Hz has been smeared out illustrates the effect of albedo flux in the rear segments on high frequency signals. The frequency resolution in all panels is 1 Hz. Characteristic error bars are shown.

noise model is seriously in error, these detections are robust (see van der Klis (1989) and Israel & Stella (1996) for further discussion of this issue). An 18 Hz feature was seen by Israel et al. (2005); it would be interesting to see if a closer analysis of the RXTE dataset reveals the 26 Hz feature. Fitting a Lorentzian profile we find for the lower frequency QPO a centroid frequency  $17.9 \pm 0.1$  Hz,  $Q$  of 10, and integrated RMS fractional amplitude  $4.0 \pm 0.3$  %. For the higher frequency QPO we find a centroid frequency  $25.7 \pm 0.1$  Hz,  $Q$  of 9 and an integrated RMS fractional amplitude of  $5.0 \pm 0.3$  %.

The weaker 30 Hz feature does not meet the  $3\sigma$  criterion at either 1 Hz or 2 Hz resolution. As such we are unable to make a robust confirmation of the 30 Hz QPO suggested by Israel et al. (2005), despite higher count-rates. One might boost the significance of this feature by combining RXTE and RHESSI datasets; but since the time window reported by Israel et al. (2005) is different, some caution is warranted.

### 3. DISCUSSION

The strong rotational-phase dependence of the QPOs in the tail of the SGR 1806–20 hyperflare provides compelling evidence that all of the oscillations are associated with particular regions of the stellar surface or magnetosphere. In this section we discuss the candidate mechanisms in more detail.

Israel et al. (2005) identified the 92.5 Hz QPO with the  $l = 7, n = 0$  toroidal mode of the crust. This in-

terpretation was supported by the apparent detection of a QPO at 30 Hz, the expected frequency of the fundamental  $l = 2$  mode. Although we cannot confirm the detection of the 30 Hz QPO, the interpretation of the 92.5 Hz QPO is probably secure. If the magnetic field of  $\sim 10^{15}$  G inferred from timing analysis (Woods & Thompson 2004) is accurate, then for the 92.5 Hz QPO to be an  $l = 6$  toroidal mode the stellar mass would have to be  $< 1M_{\odot}$  for even the softest equation of state. To be an  $l = 8$  mode, the neutron star mass would have to exceed that of SGR 1900+14 by  $> 0.3M_{\odot}$  (see the discussion in Strohmayer & Watts (2005)). An alternative to the toroidal modes, with a frequency in the correct range, is the crustal interface mode, but its behavior in the presence of strong magnetic fields requires further study (Piro & Bildsten 2005; Piro 2005).

The detection of a QPO at 626.5 Hz is exciting, as there are several crustal modes that could have frequencies in this range. The most likely candidate is the  $n = 1$  toroidal mode; the detected frequency agrees extremely well with the most recent models (Piro 2005). This would be fascinating in terms of energetics; the energy required to excite  $n > 0$  modes is orders of magnitude larger than that required to excite an  $n = 0$  mode, a testament to the strength of this particular flare. Other candidates include the crustal spheroidal modes or the crust/core interface modes (McDermott et al. 1988), although the effect of a strong magnetic field on these modes remains to be calculated. If this mode is indeed a higher radial overtone, it could allow us to determine the depth at which the fracture occurred in the crust.

The nature of the 18 and 26 Hz QPOs is less clear. The frequencies are too low for the fundamental crustal toroidal mode unless the neutron star parameters are very extreme. A torsional mode of the core, restored by the poloidal magnetic field (Thompson & Duncan 2001), was suggested by Israel et al. (2005) as a candidate mechanism for the 18 Hz QPO. Whether such modes could explain both of the QPOs is a matter for further study.

The fact that the various QPOs are strongest at different times, suggests that we may be seeing two separate fracture/reconnection events. The first, associated with the main flare, excites the 626.5 Hz QPO. The second, associated with the late time boost in unpulsed emission, excites the 92.5 Hz QPO. The idea that we might be seeing separate fracture sites is given additional weight by the observation that the two QPOs are strongest at different rotational phases. Such sequential rupturing is often observed in terrestrial seismology. It is interesting that the 18 and 26 Hz QPOs are strongest at the rotational phase where the 92.5 Hz QPO subsequently appears. One might speculate that the magnetospheric oscillations associated with the low frequency QPOs (which are triggered by the main flare) slowly weaken the crust at this point and trigger the second fracture.

Understanding the means by which the modes couple to the magnetic field, and hence modulate the X-ray lightcurve, is now critical. The fact that the modes appear in different energy bands is intriguing, as is the fact that the 626.5 Hz QPO appears at a rotational phase when a large part of the surface should be obscured by the trapped fireball. Much theoretical effort is clearly still required, but prospects for neutron star asteroseismology are bright.

We would like to thank Brian Dennis, Kim Tolbert, David Smith and in particular Richard Schwartz for advice on RHESSI data analysis. ALW acknowledges sup-

port from a National Research Council Resident Research Associateship.

#### REFERENCES

- Blaes, O. et al. 1989, ApJ, 343, 839  
 Boggs, S. et al. 2004, GCN Circ., 2936  
 Buccheri, R. et al. 1983, A&A, 128, 245  
 Duncan, R.C. 1998, ApJ, 498, L45  
 Duncan, R.C., & Thompson, C. 1992, ApJ, 392, L9  
 Flowers, E., & Ruderman, M.A. 1977, ApJ, 215, 302  
 Hurley, K. et al. 1999, Nature, 397, 41  
 Hurley, K. et al. 2005, Nature, 434, 1098  
 Israel, G., & Stella, L. 1996, ApJ, 468, 369  
 Israel, G. et al. 2005, ApJ, 628, L53  
 Lin, R.P. et al. 2002, Solar Physics, 210, 3  
 Mazets, E.P. et al. 1979, Nature, 282, 587  
 McConnell, M.L. et al. 2004, Advances in Space Research, 34, 462  
 McDermott, P.N. et al. 1988, ApJ, 325, 725  
 Palmer, D.M. et al. 2005, Nature, 434, 1107  
 Park, J. et al. 2005, Science, 308, 1139  
 Piro, A.L. 2005, ApJ, 634, L153  
 Piro, A.L., & Bildsten, L. 2005, ApJ, 619, 1054  
 Schumaker, B.L., & Thorne, K.S. 1983, MNRAS, 203, 457  
 Schwartz, S.J. et al. 2005, ApJ, 627, L129  
 Strohmayer, T.E. 1991, ApJ, 372, 573  
 Strohmayer, T.E., & Markwardt, C.B. 1999, ApJ, 516, L81  
 Strohmayer, T.E., & Watts, A.L. 2005, ApJ, 632, L111  
 Terasawa, T. et al. 2005, Nature, 434, 1110  
 Thompson, C., & Duncan, R.C. 1995, MNRAS, 275, 255  
 Thompson, C., & Duncan, R.C. 2001, ApJ, 561, 980  
 van der Klis, M. 1989, in *Timing Neutron Stars*, NATO ASI, series C, eds. H.Ögelmann & E.P.J. van den Heuvel, Dordrecht: Reidel, p.27  
 Willis D.R. et al. 2005, A&A, 439, 245  
 Woods, P.M., & Thompson, C. to appear in *Compact Stellar X-ray Sources*, eds. W.H.G. Lewin and M. van der Klis, Cambridge University Press, astro-ph/0406133